luo, S., Wang, X-J., Chen, H., Yu, Z-J., Lou, W-Y., Xia, L. M., Lou, B-Y., Liu, X-F., Kang, P., Lennox, A., & Wu, Q-A. (2018). Structural Design of Conjugated Poly (ferrocene-phenanthroline) for Photocatalytic Hydrogen Evolution from Water. *ChemPhotoChem*, *2*(9), 791-795. https://doi.org/10.1002/cptc.201800070

Structural Design of Organic Conjugated Poly(ferrocene-phenantholine) for Photocatalytic Hydrogen Evolution from Water

Shu-Ping Luo, * [a] Xiao-Jing Wang, [a] Hao Chen, [a] Zhe-Jian Yu, [a] Wen-Ya Lou, [a] Liang-Min Xia, [a] Bai-Yang Lou, [a] Xue-Fen Liu, [b] Peng Kang, [c] Alastair J. J. Lennox [d] and Qing-An Wu * [a]

Abstract: The discovery of highly efficient photocatalysts for water-splitting remains a challenge of high importance. Here, we report a series of novel organic conjugated polymers (OCPs) that contain complexed non-noble metals for photocatalytic hydrogen evolution. The conjugated chromophore polymers were synthesized by a Heck coupling between ferrocene and phenantholine derivatives, which absorb broadly, even up to the near-IR region. The photocatalyst performances were investigated for hydrogen evolution using $Fe_3(CO)_{12}$ as a water reduction catalyst. H_2 evolution rates up to 212.4 μmolh^{-1}, with an apparent quantum yield of 10.3% at 380 nm, were obtained with a photocatalyst polymer based on alternating ferrocene and 4,7-bisphenyl-1,10-phenanthroline units. The high activity is likely due to favorable electron transfer and coordination of $Fe_3(CO)_{12}$ with phenanthroline in the supramolecular OCPs.

Limited fossil fuel reserves and serious environmental pollution require an urgent search for renewable green power sources.[1] Hydrogen gas generated by photochemical water splitting is a highly attractive option. To realize a light-driven hydrogen-based economy, the development of efficient, safe and cheap photocatalysts are required, but still remains a big challenge. During the past few decades, inorganic materials based on metals with d^0 or d^{10} electronic configurations have been developed for water splitting, such as TiO_2,[2] ZrO_2,[3] CdS[4] and so on.[5] But their relatively limiting properties has impelled the development of metal-free photocatalysts for water splitting. Graphitic carbon nitride polymer (g-C_3N_4) was discovered by Xinchen Wang's group in 2009, which shows activities for photocatalytic water splitting, and opens new prospects for the search of efficient and stable organic conjugated polymer photocatalysts.[6]

The well-known advantage of organic conjugated photocatalysts is that their structures are easy to systematically adjust at the molecular level, so their physicochemical properties can be easily tuned. As a typical example, Cooper synthesized a series of pyrene-based microporous OCPs by adjusting the type and proportion of co-monomers.[7] Interestingly, the optical gap of these co-polymers was between 1.94-2.95 eV, and the hydrogen evolution rate (HER) was up to 17.4 μmolh^{-1} under visible light, rather than ultraviolet irradiation, in the presence of sacrificial agents. Subsequently, Cooper developed a series of planarized conjugated polymer photocatalysts by introducing bridging fluorene units in linear phenylenes.[8] The visible-light-driven HER rose to 116 μmolh^{-1} when Pt was added as a co-catalyst, which was further enhanced to 145 μmolh^{-1} with λ>295 nm, and the apparent quantum yield (AQY) was up to 2.3% at λ=420 nm. Recently, Hao Chen and co-workers have introduced diethynylbenzene into the backbone of linear polymers, which extended the absorption edge and showed an optimal HER of 180.7 μmolh^{-1} (AQY=4.2% at λ=420 nm) under λ>420 nm irradiation, even without a Pt co-catalyst.[9] Bipyridyl-based conjugated polymers (AQY=1.8%),[10] benzothiadiazole-based conjugated polymers (AQY=5.38%),[11] polyimide-based polymers (AQY=0.2%)[12] and other organic conjugated polymer photocatalysts were developed for photocatalytic hydrogen evolution from water,[13] but have not displayed highly efficient activities.

In 2012 we demonstrated a new non-noble metal water reduction system that employed a heteroleptic copper complex as photosensitizer (PS) and a simple, cheap, and readily available iron carbonyl complex as a water reduction catalyst (WRC).[14] We then envisioned that OCPs of copper complexes might be an efficient substitute for small copper complexes. Toward this end, we have empolyed phenanthroline derivatives with conjugating aromatic rings to facilitate structural rigidity,[15] and ferrocene, which possesses high stability, redox activity, and wide application.[16] Three novel organic conjugated polymers (OCP-1, OCP-2, OCP-3) have been prepared by a Heck coupling reaction (Figure 1).[17] We also prepared the Cu^I photosensitizer-based organic conjugated polymer (OCP-4) through coordination (Figure 1) to the metal.

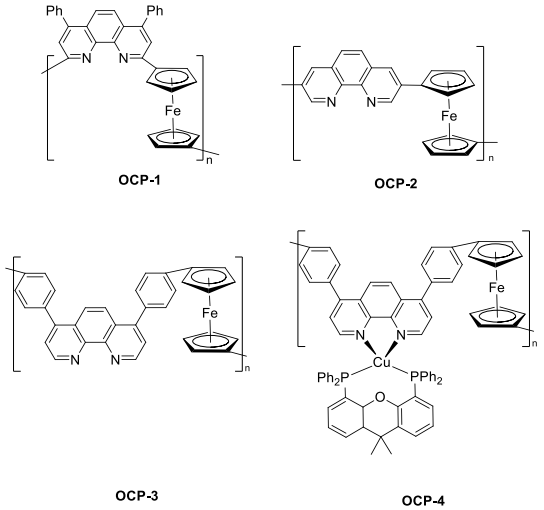

Figure 1. Structures of organic conjugated poly(ferrocene-phenantholine)

The four OCPs were obtained as black solids, and their structures were characterised by Fourier-transform infrared spectroscopy (FT-IR), scanning electron microscope (SEM), energy-dispersive spectroscopy (EDS), thermogravimetric analysis (TGA) and X-ray diffraction spectroscopy (XRD). According to the FT-IR (Figure S3-S6), the characteristic peak of ferrocene (482 cm^{-1}) was retained in the four polymers and the starting material peaks of C-Br (696 cm^{-1} - 872 cm^{-1}) disappeared. Peaks around 540 cm^{-1} could be assigned as monosubstituted compounds of cyclopentadiene. OCP-1, OCP-2

and OCP-3 were stable up to 220 ℃ under nitrogen atmosphere, as tested by TGA, but OCP-4 was weightless from 200 ℃, which might be due to copper decoordination (Figure S7). The morphology of the OCPs was then studied. The BET specific surface area of the polymers was investigated by nitrogen adsorption/desorption experiments at 77 K (Figure S8). The data of the SA_{BET} measurements are summarized in Table 1. OCP-1 showed the highest apparent SA_{BET} of 14005 cm^2/g, which is much lower than other porous[10] and microporous[18] polymers with bulky monomers. The sharp rise at high pressure regions (P/P_0=0.9−1.0) could be attributed to the presence of macropores, absorbance on external surface or textural porosity in these materials.[10] In theory , increasing SA_{BET} is advantageous to photocatalyic hydrogen evolution from water. SEM images (Figure S9) showed spherical or ellipsoidal particles were clustered, due to the paramagnetism of ferrocene, resulting in a decrease of the SA_{BET}. In addition, the X-ray diffraction (XRD) profile revealed an amorphous character as a whole, but OCP-1, OCP-2 and OCP-3 were found to show sharp and strong diffractions ranging from 15° to 20° (Figure S10), corresponding to the iron atoms of ferrocene. Surprisingly, the ordered stacking of local two-dimensional segments[10] led to broad and low intensity peaks of OCP-1 at 35° and 39°. OCP-4 showed a sharp peak at 18°, resulting from the tetrahedral crystal shape of the copper complex.[14b]

Table 1. Physical, chemical properties and hydrogen evolution rates of the OCPs

OCPs	SA_{BET}[a] cm^2/g	λ_o[b] nm	EQY[c]	Eg[d] eV	Pd[e] Wt%	$H_{2,ful}$[f] $\mu molh^{-1}$
OCP-1	14005	546	0.112	2.27	1.40	163.4
OCP-2	14796	430	0.096	2.88	2.03	187.9
OCP-3	7409	436	0.041	2.84	1.13	212.4
OCP-4	3430	625	0.007	1.98	1.05	58.1

[a] BET surface areas (SA_{BET}) were calculated from the N_2 adsorption isotherms. [b] The absorption onsets (λ_o) of these polymers were measured by diffuse reflectance UV−vis spectroscopy. [c] EQY represents emission quantum yields. [d] The optical bandgaps were calculated by the equation $E_g = 1240/\lambda_o$. [e] The residual Pd contents were measured by EDS. [f] $H_{2,ful}$ represents the hydrogen evolution rates under full-arc irradiation. Reaction conditions: 50 mg polymer, 10 mL $THF/Et_3N/H_2O$(4/3/1), 10 wt% $Fe_3(CO)_{12}$, 300 W Xe lamp.

Broad optical bandgaps and energy levels are required for effective photocatalysts. It can be clearly seen that the four polymers absorb visible light broadly (Figure 2a), and OCP-1, OCP-2 and OCP-4 reached even up to the near-IR region, facilitating the polymers to capture more visible photons. It is worth noting that the absorption range of the homopolymer of phenanthroline is only up to 500 nm,[19] which is much narrower than these OCPs, owing to the extended conjugated system introduced by ferrocene. A red-shift of OCP-1 and OCP-4 might be caused by the extended conjugated system. The absorption onset λ_o of the prepared OCPs 1-4 is 546 nm, 430 nm, 436 nm and 625 nm, respectively. Solid state fluorescence spectroscopy showed different emission peaks for the four polymers (Figure 2b). OCP-1 displayed a red-shifted peak at around 530 nm with the highest emission intensity compared to the other polymers, a decrease in photoluminescence emission intensity reduces the emission quantum yields (Table 1). OCP-4 exhibited the weakest fluorescence intensity probably due to the quenching of the Cu^I photosensitizers by ferrocene (Figure S12, K_{SV} was 2066 L/mol according to the Stern-Volmer equation). The fluorescence life-time of OCP-3 (Figure S13, τ_1=1.26 ns, τ_2=3.38 ns, τ_3=9.11 ns) was estimated by time correlated single photon counting.

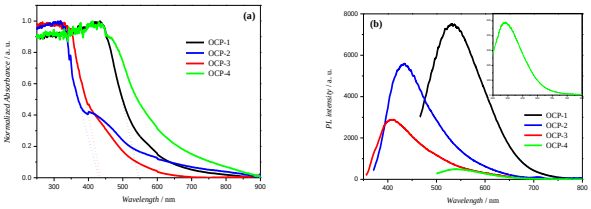

Figure 2. a) UV-vis absorption spectra of OCPs measured in the solid state powder. b) Photoluminescence spectra of OCPs measured in the solid state powder with the excitation wavelengths at 455nm, 359nm, 346nm, 473nm respectively (Figure S11).

Photocatalytic hydrogen evolution experiments were carried out with OCPs in the presence of triethylamine (TEA) as a sacrificial agent (SA) (Figure S16). We found that the rate of hydrogen evolution increased with an increase of polymer, without additional metal cocatalyst (Figure 3a), and the highest hydrogen evolution rate came from OCP-3 with up to 53.1 $\mu molh^{-1}$ under full-arc illumination (Figure 3a). In general, Pt, Ru and other nobel metals have been used as cocatalysts in previous reports,[20] but the non-noble metal $Fe_3(CO)_{12}$ was introduced as a co-catalyst in our system. The results showed that the hydrogen evolution rate decreased as $Fe_3(CO)_{12}$ increases (Figure 3b): the iron atoms in the ferrocene units may coordinate to carbonyl groups introduced by the co-catalyst and destroy the molecular structure.[21] The photocatalytic hydrogen evolutions of OCP-1, OCP-2 and OCP-3 were similar when the polymer content was in low concentration (10 mg and 30 mg). When the polymer content increased to 50 mg, the hydrogen evolution rates of OCP-2 and OCP-3 increased exponentially, while OCP-1 remained unchanged (Figure 3a). As the $Fe_3(CO)_{12}$ content increases, hydrogen evolution rates of OCP-2 and OCP-3 decrease less rapidly than OCP-1. A possible reason why OCP-2 and OCP-3 had better hydrogen production activity compared to OCP-1 is that ferrocene is not positioned in the second position of phenanthroline and is less affected by the coordination with $Fe_3(CO)_{12}$. Employing 10 wt% $Fe_3(CO)_{12}$ as the co-catalyst, a fourfold higher HER of 212.4 $\mu molh^{-1}$ was achieved under the optimized reaction conditions for OCP-3 (Figure 3b). OCP-4 did not show good activity as photons were absorbed by the polymer, rather than the Cu^I complexes, and thus the bidentate ligands appear to be best reserved for coordination of the iron co-catalyst to form a supramolecular polymer structure. There was no correllation between the hydrogen evolution performance of OCPs and BET surface area, residual palladium content or the emission quantum yields

(Table 1), but were closely related to the electronic distribution. When phenyl was used as the "bridge" between phenanthroline and ferrocene, the spatial twist angle between phenanthroline and ferrocene was small, resulting in the electronic cloud distribution of the HOMO and LUMO states concentrating on ferrocene and phenanthroline, respectively. The moderate fluorescence intensity could be the result of a more efficient charge separation.[22] The hydrogen evolution of OCP-3 is higher than OCP-1 and -2, despite the emission quantum yield being lower (0.041 vs 0.112 and 0.096, respectively). This may be due to the incident light being absorbed directly by the material for H_2 production, as well as being emitted. In addition, the HER of OCP-3 was nine times higher than that of porous conjugated polymers and almost two times higher than P-5 (Table S3),[10] which can be attributed to the structural rigidity of the phenanthroline derivatives and the redox activity of the ferrocene with cylindrical structure.

The HER of OCP-3 under different incident light wavelengths was examined (Figure 4a). We found that the HER decreased as the wavelength increases in the visible light range, and the highest hydrogen evolution rate (124.8 $\mu molh^{-1}$) coincided with the absorption intensity of OCP-3. The best AQY of OCP-3 under λ=380 nm illumination was up to 10.3%. To investigate the structural change of OCP-3 in the reaction, the FT-IR analysis of this material under different conditions was measured (Figure 4b). When $Fe_3(CO)_{12}$ was added in the reaction mixture, new carbonyl peaks around 2027 cm^{-1} appeared in the FT-IR spectrum of OCP-3, which indicates that a supramolecular polymer with two different iron complexes is formed (Figure 5). After irradiation for 1.5 h, the peak intensity of the carbonyls reduced, indicating the structure of OCP-3 is kept stable and only carbonyl was slowly destroyed. In addition, when $Fe_3(CO)_{12}$ was re-added, the iron carbonyl coordinated with OCP-3 and four additional efficient cycles were observed under full-arc illumination (Figure 4c). The slight decrease in hydrogen evolution rate over the consecutive cycles may be due to the newly added carbonyl groups from $Fe_3(CO)_{12}$ partially coordinating to the ferrocene units of OCP-3.

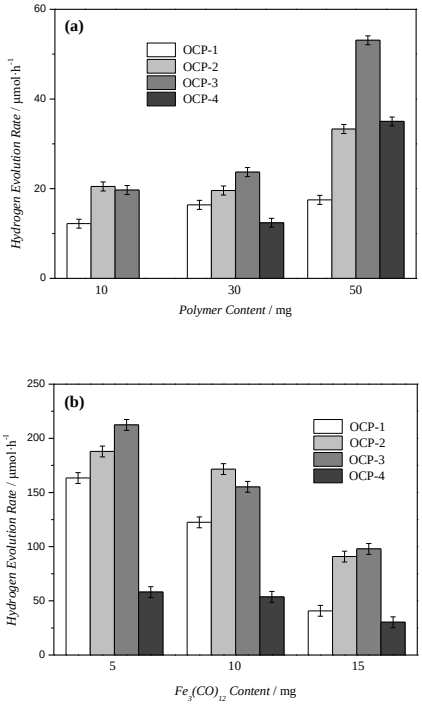

Figure 3. Effect of catalyst amount (a) and co-catalyst content (b) on the H_2 production activity of under full-arc irradiation. The data of the blank tests and hydrogen production of $Fe_3(CO)_{12}$ without OCPs were listed in the Figure S17. All gas volumes recorded in this communication have been reduced by the blank volume in the absence of OCP.

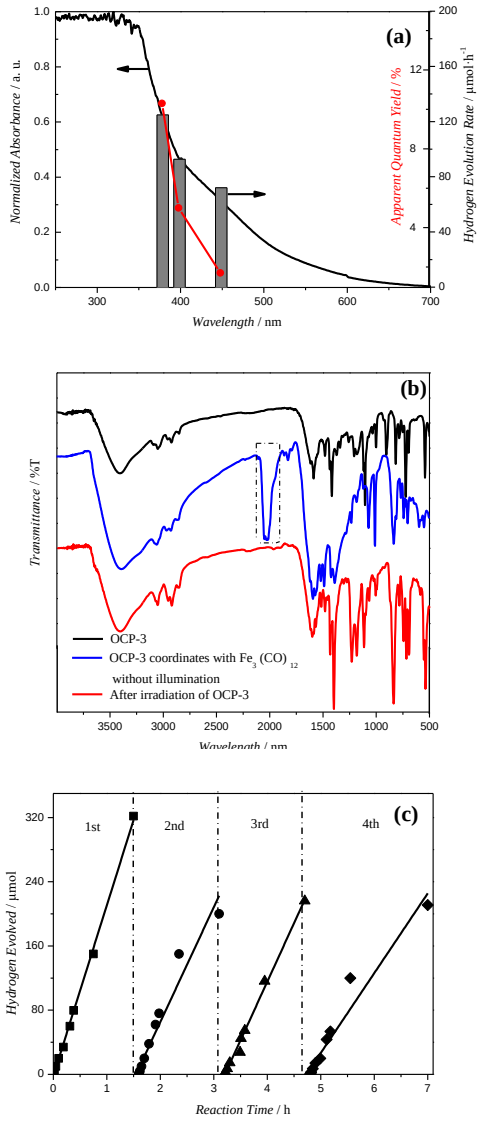

Figure 4. a) Wavelength-dependent hydrogen evolution rate and apparent quantum yields for OCP-3. b) FT-IR spectra of OCP-3, OCP-3 coordinates with $Fe_3(CO)_{12}$ without illumination at room temperature and after irradiation under full-arc light for 1.5 h in a tetrahydrofuran/triethylamine/water mixture. c) Stability test using OCP-3 with 5 wt% $Fe_3(CO)_{12}$ from water containing 12.5 vol% triethylamine under full-arc illumination.

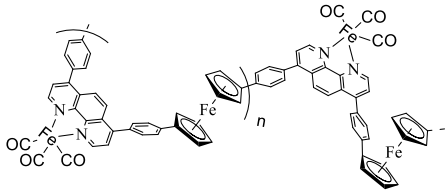

Figure 5. The plausible supramolecular structure of OCP-3 with $Fe_3(CO)_{12}$

To gain insightful information about the relative HOMO and LUMO energy levels, we analysed the best and worst performing polymers for hydrogen production by DFT calculations (OCP-1 (n=1) and OCP-3 (n=1)) (Table S2). When the phenanthroline and ferrocene are linked without bridging spacers (OCP-1), the dihedral angles between phenanthroline and ferrocene are almost right angles. Fusing of phenanthroline and ferrocene by the introduction of a benzene bridge (OCP-3), lowers the phenanthroline and ferrocene torsion angle and increases the rigidity. Extended planarized units in polymers has been shown to improve hydrogen evolution activity.[8] To further research the energy band structures of the OCP-1, OCP-2 and OCP-3 polymers, cyclic voltammetry (CV) measurements were conducted (Figure S14). The three polymers have similar energy levels and band gaps (Figure S15), as the structure of the co-monomers does not change much. The excellent hydrogen production performance of OCP-3 indicates that the energy band gap of OCP-3 is more suitable for the water reduction reaction and this data provides important evidence that explains the outstanding performance of OCP-3 over OCP-1 and OCP-2.

In conclusion, a series of organic conjugated polymers was designed and synthesized by Heck cross-coupling between ferrocene and phenanthroline derivatives. Their morphology, optical properties and performance of photocatalytic hydrogen evolution from water was explored. When bridging spacers were introduced between the phenanthroline and ferrocene, electron transfer is facilitated and H_2 evolution efficiencies up to 212.4 $\mu molh^{-1}$ were recorded, which indicates the importance of electron transfer. We will further research the hydrogen production of OCP-3 and its derivatives.

Acknowledgements

Financial support by the National Natural Science Foundation of China (No. 21376222) and the Natural Science Foundation of Zhejiang Province (No. LY18B060011). Thanks to Prof. Dr. Cheng Zhang for help in the electrochemical measurements.

Keywords: Conjugation polymer • Hydrogen evolution • Photocatalysis • Supramolecular polymer

[1] a) L. Gibson, E. N. Wilman, W. F. Laurance, *Trends Ecol. Evol.* **2017**, *32*, 922-935; b) A. H. Cavusoglu, X. Chen, P. Gentine, O. Sahin, *Nat. Commun.* **2017**, *8*, 1-9.

[2] a) H. Zhang, J. M. Cai, Y. T. Wang, M. Q. Wu, M. Meng, Y. Tian, X. G. Li, J. Zhang, L. R. Zheng, Z. Jiang, J. L. Gong, *Appl. Catal., B* **2018**, *220*, 126-136; b) Y. T. Liao, Y. Y. Huang, H. M. Chen, K. Komaguchi, C. H. Hou, J. Henzie, Y. Yamauchi, Y. Ide, K. C. W. Wu, *ACS Appl. Mate. Interfaces* **2017**, *9*, 42425-42429; c) N. R. Khalid, M. Liaqat, M. B. Tahir, G. Nabi, T. Iqbal, N. A. Niaz, *Ceram. Int.* **2018**, *44*, 546-549.

[3] a) K. Sayama, H. Arakawa, *J. Phys. Chem* **1993**, *97*, 531-533; b) Y. S. Lai, H. H. Lu, Y. H. Su, *ACS Sustainable Chem. Eng.* **2017**, *5*, 7716-7722; c) W. H. Li, X. W. Nie, X. Jiang, A. F. Zhang, F. S. Ding, M. Liu, Z. M. Liu, X. W. Guo, C. S. Song, *Appl. Catal., B* **2018**, *220*, 397-408.

[4] a) Q. X. Peng, D. Xue, S. Z. Zhan, C. L. Ni, *Appl. Catal., B* **2017**, *219*, 353-361; b) Y. X. Xu, R. T. Chen, Z. Li, A. L. Li, H. X. Han, C. Li, *ACS Appl. Mate. Interfaces* **2017**, *9*, 23230-23237; c) Y. G. Lei, C. Yang, J. H. Hou, F. Wang, S. X. Min, X. H. Ma, Z. L. Jin, J. Xu, G. X. Lu, K.-W. Huang, *Appl. Catal., B* **2017**, *216*, 59-69.

[5] K. Maeda, *J. Photochem. Photobiol., C* **2011**, *12*, 237-268.

[6] a) X. C. Wang, K. Maeda, A. Thomas, K. Takanabe, G. Xin, J. M. Carlsson, K. Domen, M. Antonietti, *Nature Mater.* **2008**, *8*, 15712-15727; b) D. D. Zheng, G. G. Zhang, Y. D. Hou, X. C. Wang, *Appl. Catal., A* **2016**, *521*, 2-8; c) Z. A. Lan, G. G. Zhang, X. C. Wang, *Appl. Catal., B* **2016**, *192*, 116-125.

[7] R. S. Sprick, J. X. Jiang, B. Bonillo, S. Ren, T. Ratvijitvech, P. Guiglion, M. A. Zwijnenburg, D. J. Adams, A. I. Cooper, *J. Am. Chem. Soc.* **2015**, *137*, 3265-3270.

[8] R. S. Sprick, B. Bonillo, R. Clowes, P. Guiglion, N. J. Brownbill, B. J. Slater, F. Blanc, M. A. Zwijnenburg, D. J. Adams, A. I. Cooper, *Angew. Chem. Int. Ed.* **2016**, *55*, 1792-1796.

[9] X. H. Zhang, X. P. Wang, J. Xiao, S. Y. Wang, D. K. Huang, X. Ding, Y. G. Xiang, H. Chen, *J. Catal.* **2017**, *350*, 64-71.

[10] L. W. Li, Z. X. Cai, Q. H. Wu, W. Y. Lo, N. Zhang, L. X. Chen, L. P. Yu, *J. Am. Chem. Soc.* **2016**, *138*, 7681-7686.

[11] C. Yang, B. C. Ma, L. Z. Zhang, S. Lin, S. Ghasimi, K. Landfester, K. A. I. Zhang, X. C. Wang, *Angew. Chem. Int. Ed. Engl.* **2016**, *55*, 9348-9352.

[12] S. Chu, Y. Wang, C. C. Wang, J. C. Yang, Z. G. Zou, *Int. J. Hydrogen Energy* **2013**, *38*, 10768-10772.

[13] a) S. W. Wen, A. L. Qu, S. K. Wu, Y. F. Cui, X. M. Xu, *Appl. Catal., A* **2017**, *542*, 336-342; b) Y. Huang, B. Zhang, *Angew. Chem. Int. Ed.* **2017**, *56*, 14804-14806; c) X. Huang, H. Y. Yao, Y. T. Cui, W. Hao, J. Zhu, W. Xu, D. B. Zhu, *ACS Appl. Mate. Interfaces* **2017**, *9*, 40752-40759.

[14] a) S. P. Luo, E. Mejía, A. Friedrich, A. Pazidis, H. Junge, A.-E. Surkus, R. Jackstell, S. Denurra, S. Gladiali, S. Lochbrunner, M. Beller, *Angew. Chem. Int. Ed.* **2013**, *52*, 419-423; b) E. Mejía, S. P. Luo, M. Karnahl, A. Friedrich, S. Tschierlei, A. E. Surkus, H. Junge, S. Gladiali, S. Lochbrunner, M. Beller, *Chem. Eur. J.* **2013**, *19*, 15972-15978; c) A. J. J. Lennox, S. Fischer, M. Jurrat, S. P. Luo, N. Rockstroh, H. Junge, R. Ludwig, M. Beller, *Chem. Eur. J.* **2016**, *22*, 1233-1238; d) Y.-Y. Sun, H. Wang, N.-Y. Chen, A. J. J. Lennox, A. Friedrich, L.-M. Xia, S. Lochbrunner, H. Junge, M. Beller, S. Zhou, S.-P. Luo, *ChemCatChem* **2016**, *8*, 2340-2344; e) N. Y. Chen, L. M. Xia, A. J. J. Lennox, Y. Y. Sun, H. Chen, H. M. Jin, H. Junge, Q. A. Wu, J. H. Jia, M. Beller, S. P. Luo, *Chem. Eur. J.* **2017**, *23*, 3631-3636.

[15] a) M. Tamura, H. Ogata, Y. Ishida, Y. Takahashi, *Tetrahedron Lett.* **2017**, *58*, 3808-3813; b) S. Schöne, T. Radoske, J. März, T. Stumpf, M. Patzschke, A. Ikeda-Ohno, *Chem. Eur. J.* **2017**, *23*, 13574-13578; c) F. H. Li, Z. Yang, H. Q. Weng, G. Chen, M. Z. Lin, C. Zhao, *Chem. Eng. J.* **2018**, *332*, 340-350.

[16] a) J. H. Jia, Y. Z. Li, J. R. Gao, *Dyes Pigments* **2017**, *137*, 342-351; b) H. K. Li, W. W. Chi, Y. J. Liu, W. Yuan, Y. W. Li, Y. F. Li, B. Z. Tang, *Macromol. Rapid Commun.* **2017**, *38*, 1700075; c) Z. Liu, L. Feng, X. R. Su, C. Y. Qin, K. Zhao, F. Hu, M. J. Zhou, Y. Y. Xia, *J. Power Sources* **2018**, *375*, 102-105.

[17] C. Díaz, D. Alzate, R. Rodríguez, C. Ochoa, C. A. Sierra, *Synth. Met.* **2013**, *172*, 32-36.

[18] R. S. Sprick, B. Bonillo, M. Sachs, R. Clowes, J. R. Durrant, D. J. Adams, A. I. Cooper, *Chem. Commun.* **2016**, *52*, 10008-10011.

[19] W. X. Yang, T. Nakano, *Chem. Commun.* **2015**, *51*, 17269-17272.

[20] a) M. K. Bhunia, K. Yamauchi, K. Takanabe, *Angew. Chem. Int. Ed.* **2014**, *53*, 11001-11005; b) S. W. Cao, J. Jiang, B. C. Zhu, J. G. Yu, *PCCP* **2016**, *18*, 19457-19463.

[21] a) T. Nakae, M. Hirotsu, S. Aono, H. Nakajima, *Dalton Transactions* **2016**, *45*, 16153-16156; b) W. Zhong, Z. Xiao, G. Qian, X. Liu, *Electrochim. Acta* **2017**, *247*, 779-786.

[22] Y. F. Xu, N. Mao, S. Feng, C. Zhang, F. Wang, Y. Chen, J. H. Zeng, J. X. Jiang, *Macromol. Chem. Phys.* **2017**, *218*, 1700049.

We prepared a series of novel organic conjugated polymers (OCPs) via Heck reaction from ferrocene and bromized phenantholine deribatives. The designed OCPs broaden their absorption spectra up to near-IR region. Building up by the coordination bond of $Fe_3(CO)_{12}$ with phenanthroline, supramolecular polymers were formed, which promote the electron transfer and the photocatalytic H_2 evolution efficiencies up to 212.4 $\mu molh^{-1}$ were obtained.

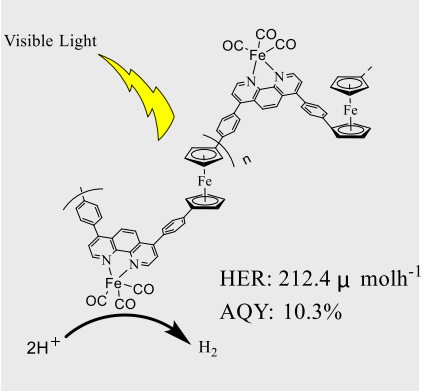

Shu-Ping Luo, Xiao-Jing Wang, Hao Chen, Zhe-Jian Yu, Wen-Ya Lou, Liang-Min Xia, Bai-Yang Lou, Xue-Fen Liu, Peng Kang, Alastair J. J. Lennox and Qin-An Wu**

Page No. 1– Page No.5

Structural Design of Organic Conjugated Poly(ferrocene-phenantholine) for Photocatalytic Hydrogen Evolution from Water